CHAPTER 1

INTRODUCTION

1.1 Background Study

According to the global energy statistical yearbook 2011 by Enerdata, the world's energy consumption rises steadily and in the year 2011, it reaches the maximum value of 13,000 Mtoe (megaton of oil equivalent). Figure 1.1 shows the increasing trend of energy consumption in the world. According to the same data, 13,200 Mtoe of energy is produced each year and from that number, the main sources of energy are still oil and natural gases. Renewable energy only accounts for 20% of the energy source where hydropower contributes about 60 % of it. Figure 1.2 shows the percentage of renewable energy production in the world.
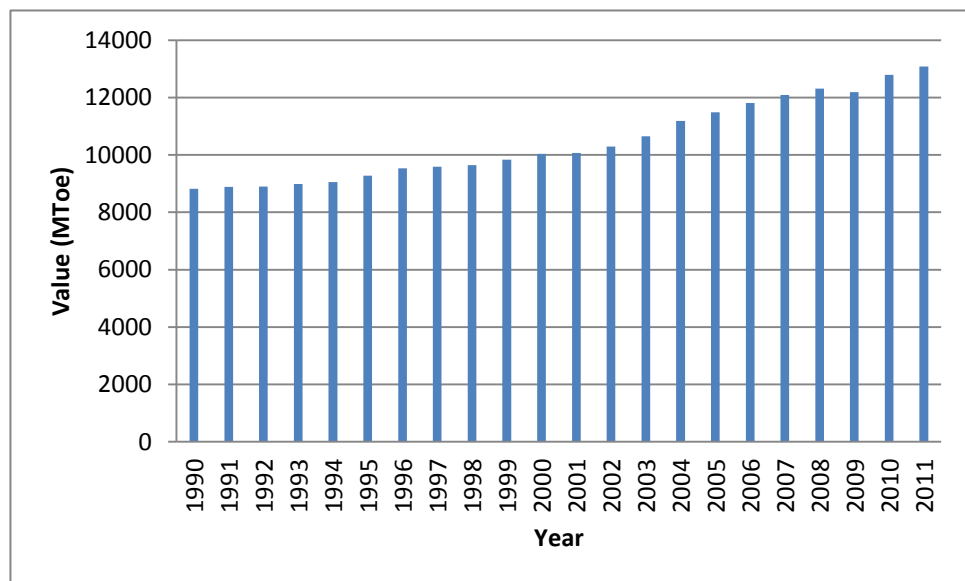
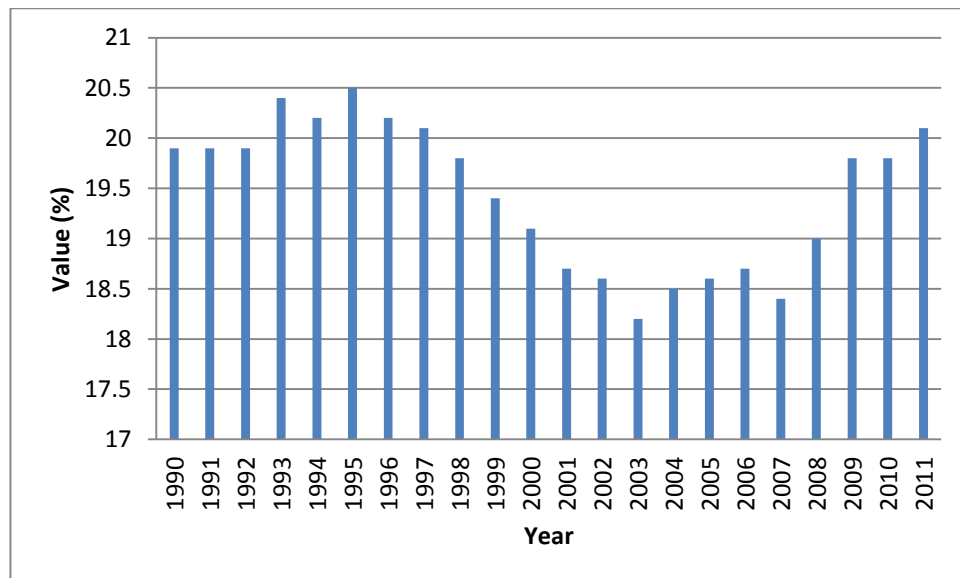

Figure 1.1 World energy consumption

Figure 1.2 Percentage of renewable energy production

The concentration of carbon dioxide (CO_2) – one of the greenhouse gases that contribute to climate change- has increased by 2.67 ppm to 395 ppm in 2012 mainly due to the burning of fossil fuels, open burning and excessive deforestation according to the new data is supplied by the National Oceanic and Atmospheric Administration (NOAA) based in the USA. One alternative to reduce CO_2 emission is the use of solar energy which is abundant. According to British Petroleum (BP) statistical review of energy production and consumption in the world in June 2012, energy production from solar power increased by 73% in 2011. This shows a growth of almost 10 times over the past 5 years. Unfortunately solar power generation only represent about 10% of the total power generation in the world. The problem with this is because the conversion efficiency of sunlight to electricity is still very low.

Traditionally, there are three types of solar cells: crystalline silicon, thin film and organic. Crystalline silicon solar cells are the major form of photovoltaic cell produced in the world. This category of solar cell shows the highest overall efficiency of approximately 22 %. But the cost of production is very high. Thin film solar cell, also called as second generation solar cell is a type of solar cell usually coated onto glass

panes. Advantages of this solar cell include the reduced weight of the solar cell compared to crystalline silicon solar cells, less amount of material used and high transparency. But the downside of this solar cell is that the efficiency is not as good as first generation solar cell. The last type of photovoltaic cell is the organic solar cell which has recently attracted a lot of attention. Organic solar cell uses organic and polymeric materials which is conductive to convert sunlight to electron. Some of the benefits are low cost of production, flexible and easy to process. Unfortunately, the conversion efficiency is extremely low.

The highest ever reported efficiency for a solar cell is 37.8 % reported by Spectrolab a subsidiary of Boeing. In the invention, the company employs a multi-junction solar cell where different semiconductor materials were used. Another material that is often used in solar cells and has high conversion efficiency is silicon. A black silicon solar cell can achieve efficiency as high as 18.7 %. Even with this improvement, it is still not enough to satisfy the world's energy consumption. Thus, all around the world people are still relying on oil and natural gas as source of energy. Solar energy production is still less than 1% of the total world production of energy. There is need for a big effort to improve the conversion efficiency of the photovoltaic cells and to bring the cost down, which is very high compared to the fossil fuels.

As one of the largest oil-producing countries, most of the research works in Malaysia are more focused on oil and gas. Thus, Malaysia is lagging behind in term of research and development in renewable energy. It has been reported that, Malaysian government has set a target that in 2001-2005, 5% out of the total energy production must come from renewable energy. Unfortunately, only 1% is achieved (M. R. Islam, 2009). One of the main reasons for this is the lack of research works and technology in green technology in Malaysia. Although Malaysia has a research institute, Solar Energy

Research Institute (SERI), dedicated in research on renewable energy, but most of their research works are on inorganic materials particularly silicon, whereas other countries already exploring the use of organic and polymer-based materials, as an alternative to silicon. The reasons behind this are that silicon is expensive whereas polymers are cheap and easily available. Also, the use of polymer in solar cells allow it to be applied in many places as it is very thin, flexible and pose no health risks.

Organic and polymeric materials are touted to be one of the most promising materials, where inorganic semiconductors have been replaced with conjugated organic semiconductors. The organic materials have significant advantages compared to inorganic materials, but big improvements need to be done. Recently, 12 % power conversion efficiency has been achieved based according to Heliatek a company developing organic solar films in Germany. The growth of the plastic solar cells results from the developments in organic synthesis and device fabrication technologies. Figure 1.3 shows the highest efficiency achieved in each year according to the types of the solar cells. As can be seen from the figure, research works for organic solar cells significantly increased since early 2000s.
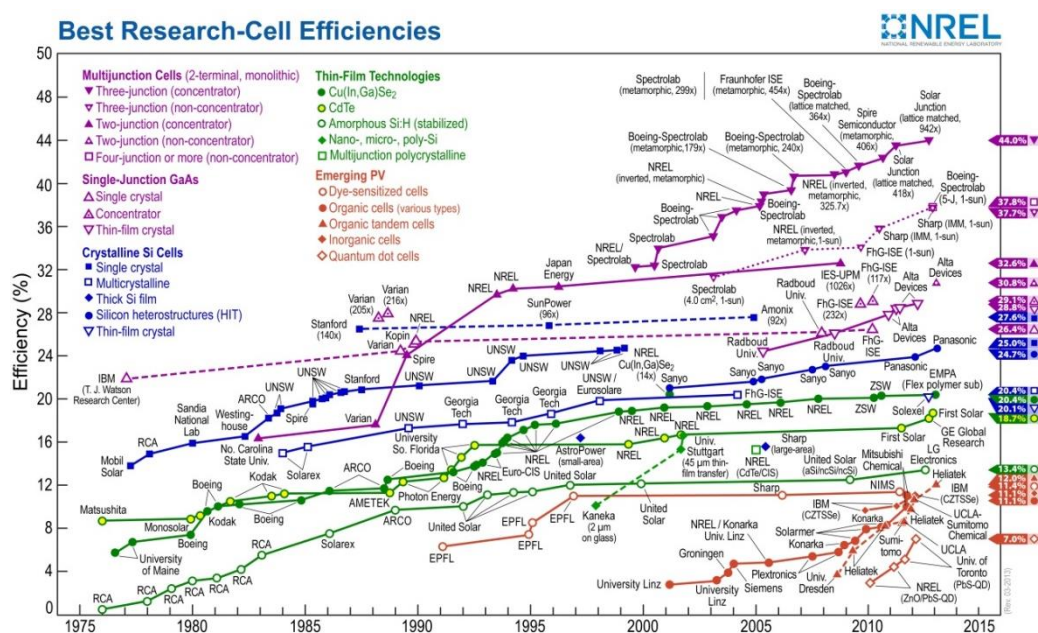

Figure 1.3 Solar cells efficiency according to the types

1.2 Problem statement

Until now, there have been many papers suggesting the use of various dopants and plasticizers in polymer electrolyte in order to significantly increase the ionic conductivity. However, the addition of some plasticizers makes the polymer electrolyte mechanically unstable either the electrolyte becomes too viscous, or the presence of air bubbles within the electrolyte or even lowering the ionic conductivity. There, however, has been little investigation in the use of liquid crystal as a plasticizer despite the interesting characteristics of it. There is a lack of experimental data in the effect of liquid crystal on the ionic conductivity and the electrochemical property which makes it difficult to make a comparison. An experiment where various parameters such as the method of fabrication and varying the concentration of liquid crystal is proposed.

1.3 Objective

The main objective of this research is to

1) Fabricate polymer electrolyte consisting of nematic liquid crystal with different methods and evaluate the performance
2) Optimize the ionic conductivity of the polymer electrolyte by varying liquid crystal concentration
3) Determine the electrochemical property such as the electronic band gap
4) Understand the physics behind the mechanism of ion or electron transport within the polymer electrolyte liquid crystal system

CHAPTER 2

BACKGROUND THEORY

In this chapter, an introduction to dye-sensitized solar cells (DSSCs) and liquid crystals (LCs) which includes the mechanism and theory of both will be given.

2.1 Dye-sensitized solar cells (DSSCs)

Dye-sensitized solar cells (DSSCs) are a type of fourth generation solar cell, which was first developed by Brian O'Regan and Michael Grätzel and the report on their finding was published in Nature in 1991 (O'Regan & Graetzel, 1991). Although the efficiency is still low compared to the existing Silicon-based solar cells which are typically around 25 %, they are very promising in replacing the conventional Si solar cells due to them having a relatively high light to energy conversion efficiency, simple fabrication procedure, low environmental impact and low fabrication.

A typical working DSSC (Figure 2.1) consists of four parts, which are (1) a transparent conducting oxide electrode, (2) a nanocrystalline TiO_2 layer with charge transfer dye on the nanoparticle surface, (3) a counter conducting electrode consisting of Pt thin layer, and (4) an electrolyte system between the two electrodes usually composed of the redox system (I_3^-/I^-). The electrolyte is one of the most important parts in a solar cell and typically, a liquid electrolyte is used in a DSSC. Unfortunately, there are some drawbacks of using liquid electrolytes such as leakage and evaporation of solvent, sealing difficulties and corrosion of electrodes. Many research works have been done to address these issues by exploring new types of electrolytes such as solid electrolytes, ionic liquids, polymer electrolytes and so on.
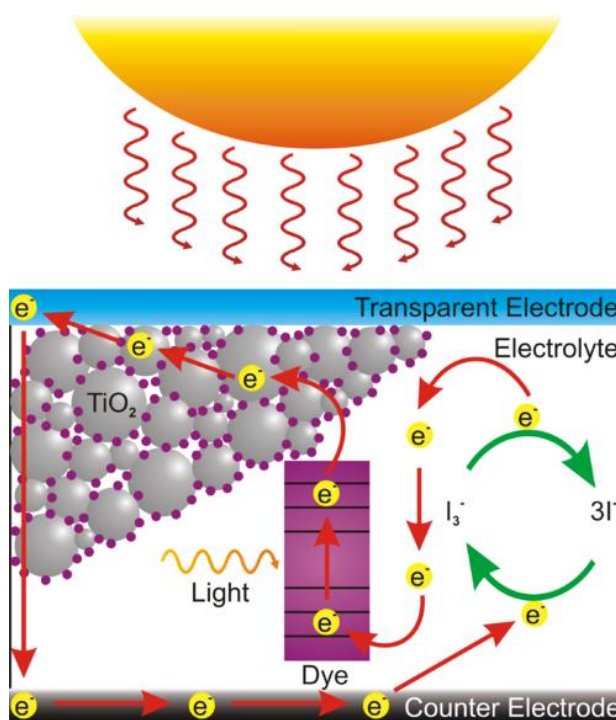
Figure 2.1 Schematic diagram of a typical DSSC

2.2 Polymer electrolyte

A conventional DSSC uses liquid electrolyte which gives the highest conductivity. Unfortunately, the use of liquid electrolyte has other disadvantages such as leakage and evaporation of solvent, difficulty in sealing and corrosion of electrodes (Nazeeruddin et al., 2005; Wang et al., 2005). To overcome this problem, an alternative is through the use of polymer electrolyte. Polymer electrolytes are electrolytes that consist of polymer/salt complex and have free ions which make them electrically conductive. Polymer electrolytes are made from salt complex mixed together with a polymer. The salt complex is responsible for making the polymer ionically conductive.

One of the earliest reports on the use of solid polymer electrolyte in DSSC applications which shown high power conversion efficiency (PCE) was by Noguira et al.

(Nogueira, Alonso-Vante, & De Paoli, 1999) in 1999. They prepared a polymer consisted of poly(epichlorohydrin-co-ethylene oxide) filled with sodium iodide (NaI) and iodine (I_2). The DSSC incorporating the polymer electrolyte showed a high ionic conductivity of 1.5 x 10^{-5} S/cm and a PCE of 2.6% at 10 mW/cm^2.

A composite can also be called a solid polymer electrolyte as has been shown by Kim et al.(J. H. Kim et al., 2004), who prepared a composite from poly(ethylene oxide dimethyl ether) (PEODME, M_w = 500 g/mol) and fumed silica. They found out the composite polymer electrolyte showed a high conversion efficiency of 4.5 % at 100 mW/cm^2. This is attributable to the excellent interaction between dye-attached TiO_2 particles and the composite polymer electrolyte. This good interaction allows for improved electrolyte diffusion into the nanopores and helps to increase the interfacial contact between the electrolyte and the electrode.

2.2.1 Mechanism of Ionic Conduction

The mechanism of ionic conduction within a polymer electrolyte is attributable to the intrachain and interchain hopping where the segmental motions of the polymer chains allow the cations to move between one coordination site to another, either on one chain or between adjacent neighboring chains. A high ionic conductivity is believed to be facilitated by the interchain hopping. Figure 2.2a and b shows the motion of cation aided by polymer's segmental motion. Ion clusters can also contribute to the ionic conduction through ion-ion interactions as shown in Figure 2.2c and d. But this type of ionic conduction is limited by the concentration of ions within the polymer host.
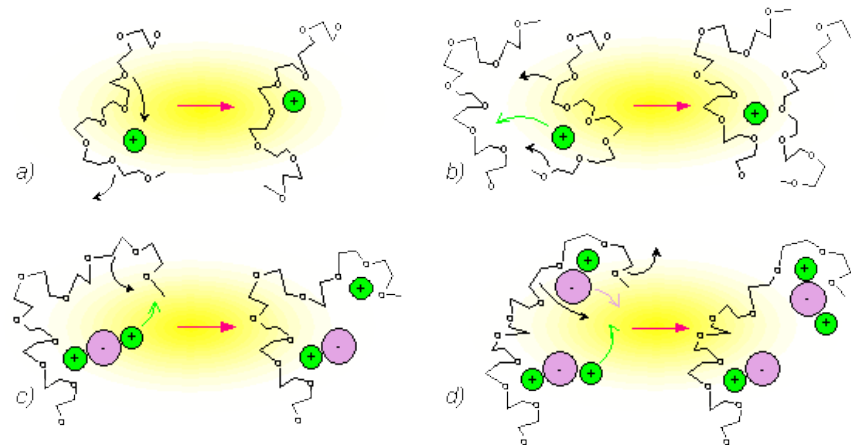
Figure 2.2 Ionic conduction mechanism of a polymer electrolyte assisted by polymer chains only and ionic cluster. a) ion hopping intrachain and b) interchain. c) ion pairs dissociates d) ion pair dissociates and pairs with another unpaired ion

A high ionic conductivity can be achieved if the polymer host is ideally in the amorphous phase or in other words, the glass transition temperature is low enough so that at room temperature it is already in amorphous state. High crystallinity in a polymer limits the performance of the polymer electrolyte (Manuel Stephan, 2006). As an example, in polyethylene oxide (PEO) and many PEO/salt mixtures, at room temperature the crystallinity is around 70-85%.

2.2.2 Factors Affecting Ionic Conductivity

One of the factors that affect the ionic conductivity of solid polymer electrolyte is the size of the cation of the salt complex. Bhattacharya et al. (Bhattacharya, Lee, Geng, Jung, & Park, 2009) found that the crystallinity decreases as the size of cations increases which proves that the ionic conductivity is related to the mobility of the ions and not due to the number of dissociated charge carriers. In the experiment, the group used complex salts with different sizes and achieved a higher ionic conductivity for the one with the largest cation size.

Another factor that can affect the ionic conductivity and thus the performance of the DSSC is the concentration of salt complex such as sodium iodide (NaI). It has been shown that the ionic conductivity of the polymer electrolyte increases proportionate to the salt concentration and once it reaches a certain concentration, the conductivity value decreases gradually (J. H. Kim, Kang, Kim, Won, & Kang, 2005). The increase in the conductivity can be attributed to the additional number of charge in the electrolyte whereas the decrease is due to the formation of ion pairs in the electrolyte (Gray, 1997; J.R. MacCallum, 1987). According to Kim et al. in the same paper, the maximum ionic conductivity obtained was 2.6×10^6 S/cm at sodium iodide to poly(butyl acrylate) (PBA) molar ratio of [Na]/[COO] = 0.1. The PCE of the DSSC employing the polymer electrolyte at the same molar ratio was 1.66 % at a solar intensity of 10 mW/cm^2.

The use of different types of polymers such as difference in chemical and/or physical properties and also with various molecular weights will also affect the ionic conductivity. Kim et al. (J. H. Kim et al., 2005) showed that there is a vast difference in PCE between PBA (M_w = 99,000 g/mol) (η = 1.66 %) and PEO (M_w = 1,000,000 g/mol) (η = 0.07 %). This vast difference in magnitude is due to (1) higher percentage of crystallinity in PEO, (2) low diffusion of chains in high-molecular weight PEO and (3) good adhesion of PBA with the electrodes.

Chen et al. (Chen, Liou, Lee, & Chen, 2010) reported that the ionic conductivity increases with increasing immersion time of the polymer into the electrolyte. In their report, polyvinylbutyral (PVB) immersed in γ-butyrolactone/N-methyl-2-pyrrolidone/LiI/I$_2$ for 10 minutes and 40 minutes have conductivities of 2.0×10^{-4} S/cm and 10.0×10^{-4} S/cm respectively. However, this is true up to a certain time after which the ionic conductivity will reach a maximum value.

Due to the solid polymer electrolyte having a low ionic conductivity compared to liquid electrolyte, researchers have been trying to improve the ionic conductivity by mixing the polymer electrolyte with other materials, changing the parameter, revising the fabrication method and many more. Recently, people start experimenting with liquid crystal as one of the materials for improving the conductivity of the polymer electrolyte.

2.3 Liquid Crystals (LCs)

Liquid crystal (LC) is a fourth state matter that combines both the properties of solid and liquid and have orientational order and sometimes positional order (Peter J. Collings, 1997). A liquid crystal molecule is consisted of a rigid part called the 'mesogen' and a flexible part. Figure 2.3 shows a typical structure of a liquid crystal where the liquid crystal is divided into two parts: spacer and mesogen.
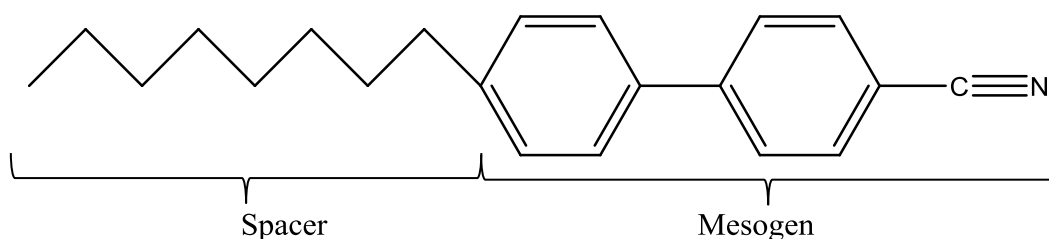

Spacer   Mesogen

Figure 2.3 Example of a typical liquid crystal structure

LCs can be categorized into two categories: thermotropic and lyotropic. Thermotropic LCs are LCs that change phases depending on the temperature whereas lyotropic LCs phases transition depends on the solvent. In this thesis, the focus is on the thermotropic LCs and the lyotropic LCs will not be discussed.

Thermotropic LCs can be divided into 3 phases namely smectic, nematic and isotropic. The closest phase to crystal is the smectic phase where the liquid crystal is very viscous and has both orientational and positional order. Increasing the temperature will turn the phase to nematic. Once it becomes nematic, the liquid crystal no longer has

the positional order but only orientational order. Lastly, as the temperature is increased further, the LC becomes isotropic which is more liquid like and does not possess orientational and positional order. Figure 2.3 below shows the transition of thermotropic liquid crystal from solid to isotropic with increasing temperature.
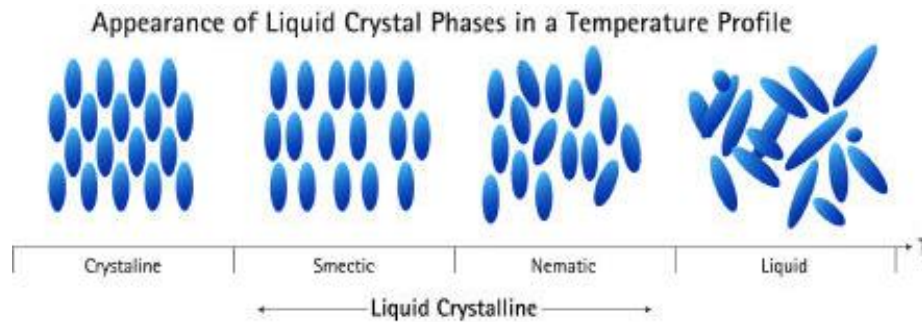

Figure 2.3 Phases of liquid crystal

2.3.1 Smectic Liquid Crystals

The smectic phase can be obtained after increasing the temperature of the liquid crystal. The smectic phase is highly ordered when compared with the nematic phase due to the phase having both positional and orientational order. The molecules within the nematic phase form a layered structure and the molecules are allowed to move freely within the layer and sometimes to different layers. The smectic phase can be viewed as a 2 D element where the mesogen aligns orthogonally and can also be tilted along the layer plane. The smectic phase can be furthered categorized into a few other types: SmA, SmC, SmB, SmF and SmI. These different types of smectic phases are characterized by different degrees of positional and orientational order.

2.3.2 Nematic Liquid Crystals

The nematic (N) liquid crystal is less ordered than the smectic phase liquid crystal which makes it less viscous than smectic phase. The phase is identified by the mesogen that aligns parallel along a director (n) as shown in Figure 2.6. The phase has orientational order but not positional order as the molecules are distributed randomly without any layers. The molecules are also able to rotate freely about their long axes. These make the nematic liquid crystal behave more like liquid than smectic phase. Although the viscosity is comparable to that of liquid, a nematic liquid crystal appears cloudy. Under an optical polarizing microscope (OPM), nematic liquid crystal shows a Schlieren texture where point defects and extinction brushes can be seen.

To better quantify the molecular orientation, the following equation was proposed:

$$S = \frac{1}{2}\langle 3cos^2\theta - 1 \rangle$$

where S is the order parameter and θ is the angle between the mesogen and the director (n). For an ideal nematic liquid crystal, the order parameter must be 1 and as it becomes isotropic, the order parameter becomes 0. Figure below shows (Figure 2.5) the representation of the angle, θ. There are several ways to determine the order parameter: deuterium nuclear magnetic resonance (NMR) and measurement of linear dichroism in UV and IR absorptions.
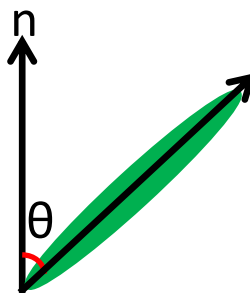

Figure 2.5 Determination of the angle between the mesogen and the director axis

2.3.4 Applications of Liquid Crystals

Liquid crystal has been used as a template for organic and inorganic materials highly ordered nature. The first report on the use of LC as a template was reported by Shirakawa et al.(Shirakawa et al., 1988), where the group succeeded in producing a film with highly aligned fibrils. The liquid crystal was us as an ordered matrix solvent assumes its alignment under applied magnetic field. This method has also been proven to increase the carrier mobility and electrical conductivity of the template material (Akagi et al., 1998; Kang, Jin, Chien, & Sprunt, 2004).

Amorphous material has a very low charge carrier mobility of about 10^{-3} cm^2/Vs or less limited its application for electronic devices. Whereas, for discotic (Bushby & Lozman, 2002; Debije et al., 2004) and smectic (Masahiro Funahashi & Hanna, 2000; M. Funahashi & Hanna, 2005) LCs alone have charge carrier mobility values of 0.4 to 0.1 cm^2/Vs which is considerably higher than that of amorphous materials. The discovery of conjugated LC and also smectic and discotic LCs at room temperature further improved the charge carrier value up to 1 cm^2/Vs. These breakthroughs allow for the development of electronic devices with high charge carrier mobility with the combination of amorphous material and liquid crystal.

The first reported work on the use of liquid crystal in solar cell was first reported by Chandra et al. (Chandra, Srivastava, & Khare, 1986). The group found that the addition of nematic n-(p-methoxy-benzylidene)p-butylanaline (MBBA) to chlorophyll electrode enhanced the photovoltage, photocurrent and photoconductivity value. Other groups have also experimented with liquid crystal as the main component in solar cell in example polymer electrolyte (H. K. Kim, Lee, Jin, & Lee, 2009; Petritsch et al., 1999; Schmidt-Mende et al., 2001).

CHAPTER 3

METHODOLOGY

3.1 Materials

Poly(vinyl alcohol) (PVA) (M_w=89,000-98,000) (Sigma Aldrich), 4'-pentyl-4-biphenylcarbonitrile (5CB) (Sigma Aldrich), potassium iodide (KI) (Merck), tetra(n-butyl)ammonium hexafluorophosphate *(*TBAHFP) (Sigma Aldrich), tetrahydrofuran (Merck) and dimethyl sulfoxide (DMSO) (Merck) were used as received.

3.2 Film Fabrication

3.2.1 Casting method

4'-pentyl-4-biphenylcarbonitrile (5CB) was added drop wise to dimethyl sulfoxide (DMSO) solution. The solution was stirred at room temperature for 1 hour. Then potassium iodide (KI) was added to the solution at stirred for another 1 hour until the salt fully dissolved. Lastly, poly(vinyl alcohol) (PVA) was added to the mixture and stirred at 100ºC for 2 hours until the solution became transparent. The resulting viscous solution is then casted in a glass petri dish and let dry at 50ºC for a few days until it formed a film. The film is cut into 1 cm x 1cm for impedance spectroscopy (IS) measurement.

3.2.2 Spin-coating Method

The spin-coating method is very similar to the casting method. Instead of casting the film in a petri dish, in this method, the resultant mixture from previous method is dropped on a glass substrate and placed in a spin coater. The thickness can be controlled by controlling the rotation speed, viscosity and amount of the sample. Once the sample was rotated, the glass substrate was placed on a hot plate at 50ºC for a few days to remove the solvent. Once the sample is dried enough, it is then used for further

characterizations.

3.3 Characterization

3.3.1 Optical Polarizing Microscopy

The phase transition temperature of the polymer electrolyte liquid crystal film was observed by using Olympus BX51-P polarising optical microscope attached to a Linkam hot stage. The sample was spin coated on a glass slide and then put under the microscope for observation. The sample was heated on the hot stage at 1℃/min and cooled at 1℃/min from room temperature to 100 ℃.

3.3.2 Differential Scanning Calorimetry

To further confirm the transition temperature of the liquid crystal inside the polymer electrolyte, differential scanning calorimetry (DSC) was used. DSC is a thermal analysis where heat is applied to measure the transition temperature and enthalpy changes of this temperature. The heat applied is constant throughout the measurement where at certain temperature where the phase transition occurs; the sample will require more or less heat to be at the same temperature as the reference. This will depend on whether it is an endothermic or exothermic process. In this experiment, the sample was placed in an aluminum sample pan and put inside the DSC together with a blank sample pan as a reference. The experiment was done at a heating rate of 10 ℃/min from 0 ℃ to 100 ℃ under argon gas. The transition temperature can be determined from the thermogram of the DSC.
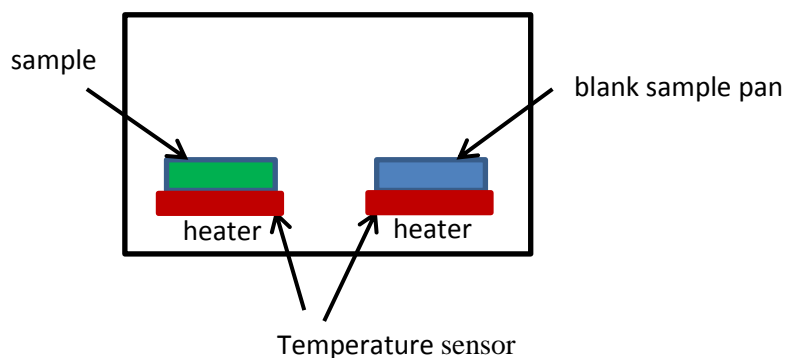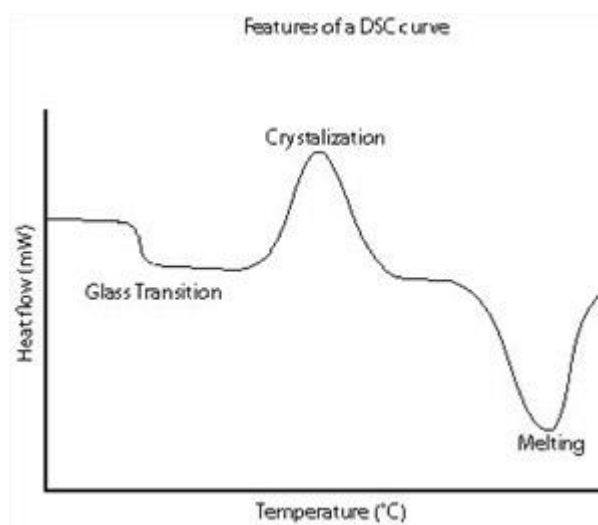
Figure 3.1 Schematic representation of DSC equipment

Figure 3.2 A typical DSC curve showing the temperature for glass transition, crystallization and melting

3.3.3 Conductivity measurement

The conductivity is measured firstly by the two electrode conductivity measurement method where impedance spectroscopy was carried out on the thin film using a HIOKI 3531-01 with the frequency range varied from 20 Hz to 1 MHz. The thin film is sandwiched between two stainless steel electrodes. Figure 3.4 shows the set up for impedance spectroscopy experiment. The two electrodes were attached to a computer with crocodile clips for data acquisition. The conductivity, σ, of each thin film is calculated using the following equation

$$\sigma = t/(R_b A) \tag{3.1}$$

where t is the thickness in cm, R_b is the bulk resistivity and A is the area of the film in cm^2. The sample holder was placed inside the temperature test chamber and the measurement was carried over a temperature range of 20 °C to 40 °C. The resistance obtained from the Cole-cole plot is taken to be the intercepting point of the frequency and the real impedance.
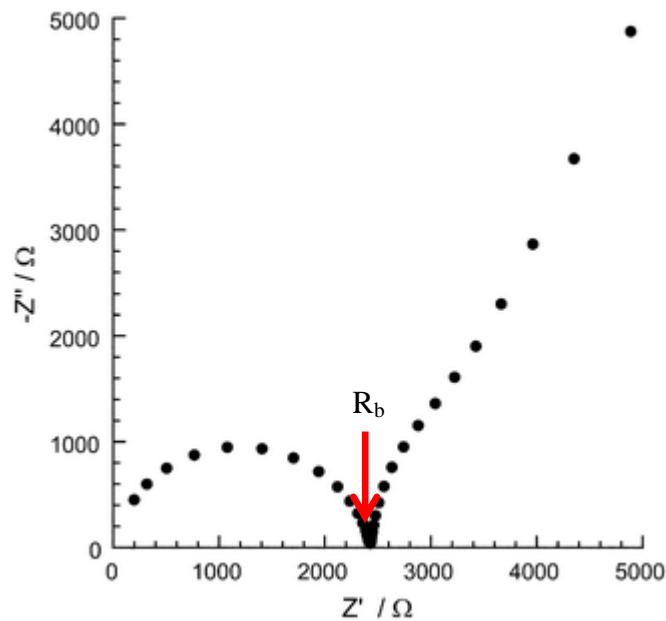

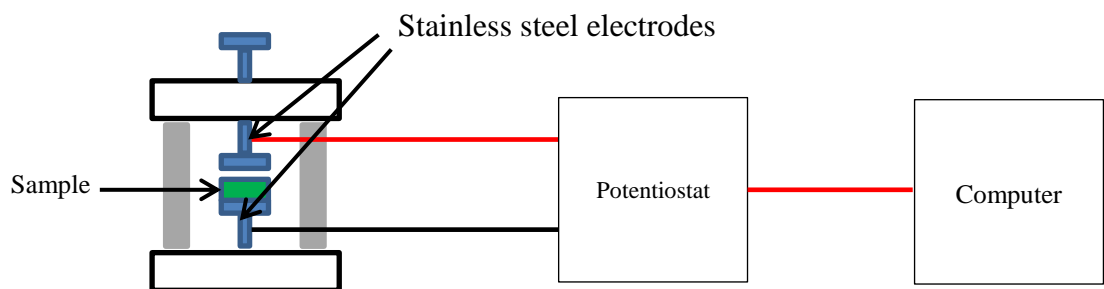Figure 3.3 A typical example of a Cole-cole plot

Figure 3.4 Diagram of an impedance spectroscopy set up

The second method to measure the conductivity is called the four-point-probe method. The frequency range of the measurement is taken from 1 Hz to 1 MHz. The following equation (Equation 3.2) is used to determine the conductivity:

$$\sigma = \frac{1}{4.5324 \times t \times R_s} \qquad (3.2)$$

where t is thickness in cm and R_s is the sheet resistivity in ohm (Ω). The resistance that is obtained from this method is the resistance of both the bulk and surface resistances. This shows that this method is more accurate than the previous method. From the impedance measurement the sample behaves as a pure resistor at low frequency. This is evident from the flat impedance response at low frequency as well as phase shift close to 0 degree.

3.3.4 Cyclic Voltammetry (CV)

Cyclic voltammetry (CV) is an electrochemical technique to examine the redox reactions of a solution where a certain voltage is applied in both forward and reverse directions giving a certain current. The scanning rate is set to be constant at all time. The resulting curve is given in Figure 3.2. The E_p and E_a correspond to LUMO and HOMO respectively. And the band gap of the material is given by the difference between E_p and E_a.
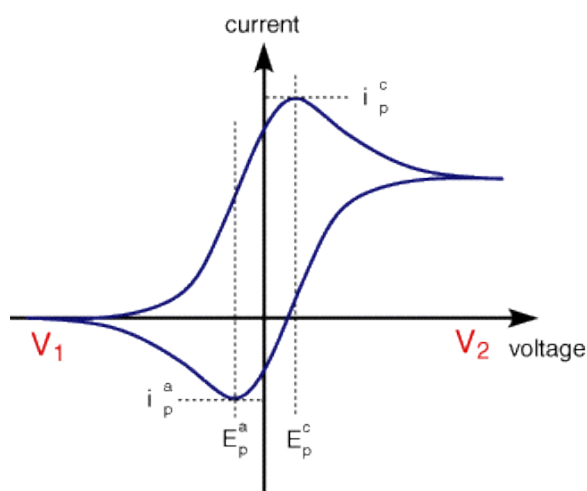

Figure 3.5 A typical cyclic voltammetry curve

The CV experiment is conducted in a three-electrode cell consisted of reference electrode (Ag/AgCl), working electrode and counter electrode at a scan rate of 50 mV/s (Gamry). Figure 3.5 below shows the set up for CV experiment where a Gamry

Potentiostat was used. The potentials were measured at room temperature with 0.1 M tetra(n-butyl)ammonium hexafluorophosphate (TBAHFP) as the supporting electrolyte in tetrahydrofuran (THF). The working electrode was prepared by spin coating the sample onto an ITO glass substrate and let dry. The determination of E_{LUMO} and E_{HOMO} can be done by using the following equation $E_{HOMO} = -[E_{red} + 4.4]$ eV and $E_{LUMO} = -[E_{oxi} + 4.4]$ eV.

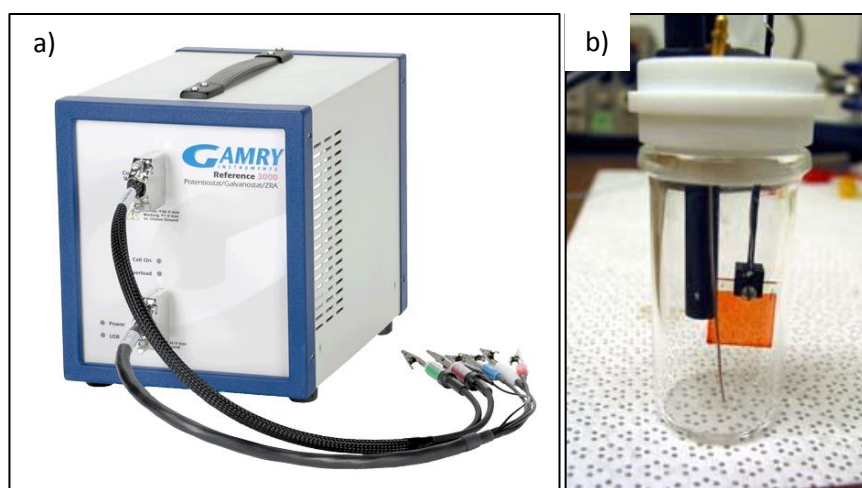Figure 3.6 Experimental a) equipment and b) set up

CHAPTER 4

RESULT AND DISCUSSION

Phase transition

The PVA-only thin film obtained is transparent, whereas the 5CB-embedded PVA thin film is cloudy and turbid. From this, it can be confirmed that the liquid crystal is embedded inside the polymer thin film. After soaking with KI solution, the membrane became yellowish in color and the color became more apparent as the concentration of KI is increased. Figure 4.1 shows the polymer membrane before and after soaking.
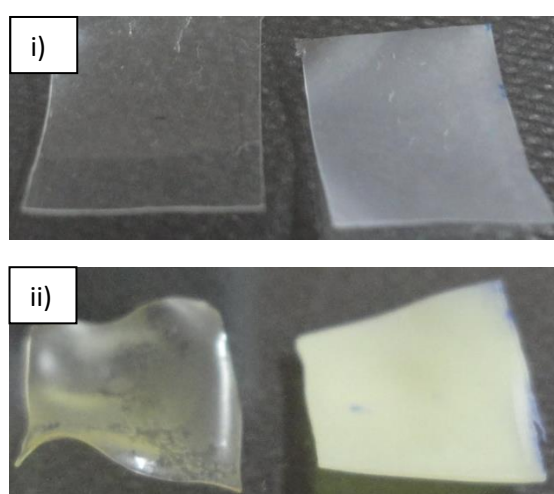

Figure 4.1 Thin film without (left) and with 15 wt% LC (right) before (i) and after (ii) soaking with KI solution

The phase change temperature for the sample prepared by casting method could not be determined due to the nature of the sample that is not transparent. The strong coloration of the sample does not allow the light from the optical polarizing microscope to pass through and thus no phase transition could be observed. In order to observe the phase transition, the sample prepared by the spin coating method was used. The nematic to isotropic temperature have been found to decrease when introduced into the polymer. For pure 5CB, the nematic to isotropic temperature is around 34.5 ℃. But the inclusion into polymer brought it down to 32~33 ℃. The figure (Figure 4.2) below shows the image of the sample at 27 ℃ and 40 ℃ (inset picture). Within the polymer electrolyte, the liquid crystal presents in the form of bubbles which is similar to polymer dispersed

liquid crystal (PDLC). As the temperature is increased, the bubbles changed from Schlieren structure to slightly transparent.
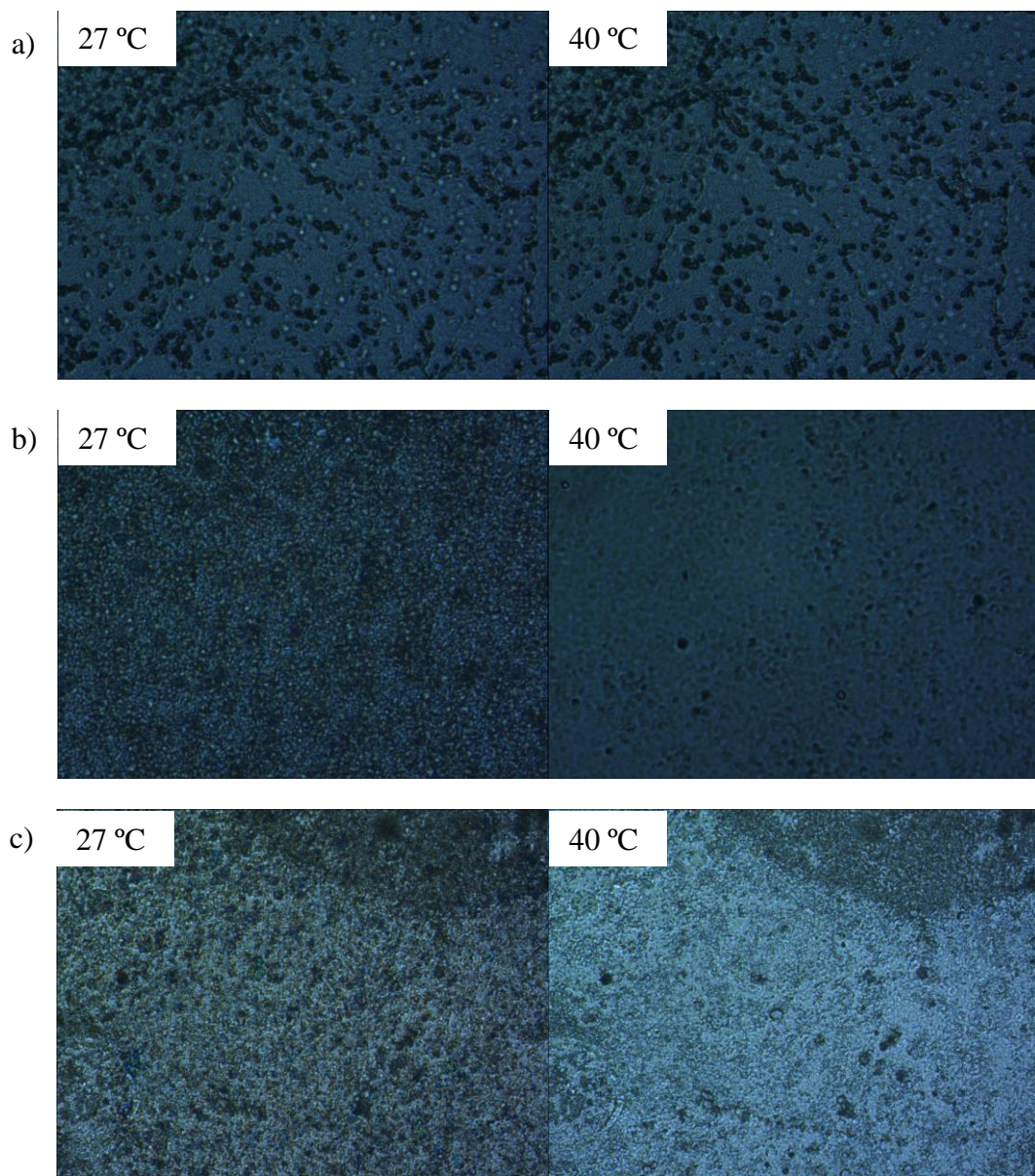

Figure 4.2 OPM images of samples at 27 ℃ and 40 ℃ of samples with a) 5 wt%, b) 10 wt% and c) 15 wt% of 5CB

Ionic conductivity measurement

Casting method

The ionic conductivity of the PELC was measured using the impedance spectroscopy method. From the method, cole-cole plot was obtained and the bulk resistance, R_b, of the sample was determined from the intercept of the semicircle arc and the real Z axis. Figure 4.3 below shows the Cole-cole plot of a PVA-only membrane soaked in KI solution at room temperature.
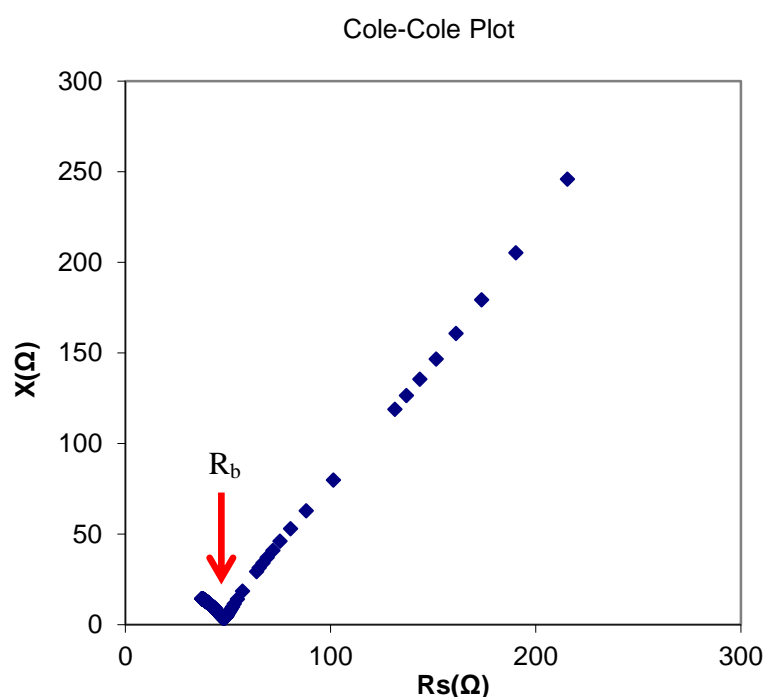
Figure 4.3 Cole-cole plot of PVA + KI (1 M)

The variation of ionic conductivity of the polymer system is as a function of concentration of KI solution is given in Figure 4.4. The polymer shows a significant increase in ionic conductivity after the introduction of 5CB up to KI concentration of 1.0 M. However, the ionic conductivity started to decrease with the increase in KI concentration above 1.0 M. This can be attributed to the increased number of KI molecules within the polymer which significantly reduced free spaces for cation movement that is responsible for high ionic conductivity. The highest conductivity

obtained is for sample with 10 wt % of 5CB at KI concentration of 1.0 M which shows conductivity of 2.42 x 10^{-4} S/cm. For the same KI concentration, the PVA-only membrane only showed a conductivity of 1.45 x 10^{-4} S/cm.
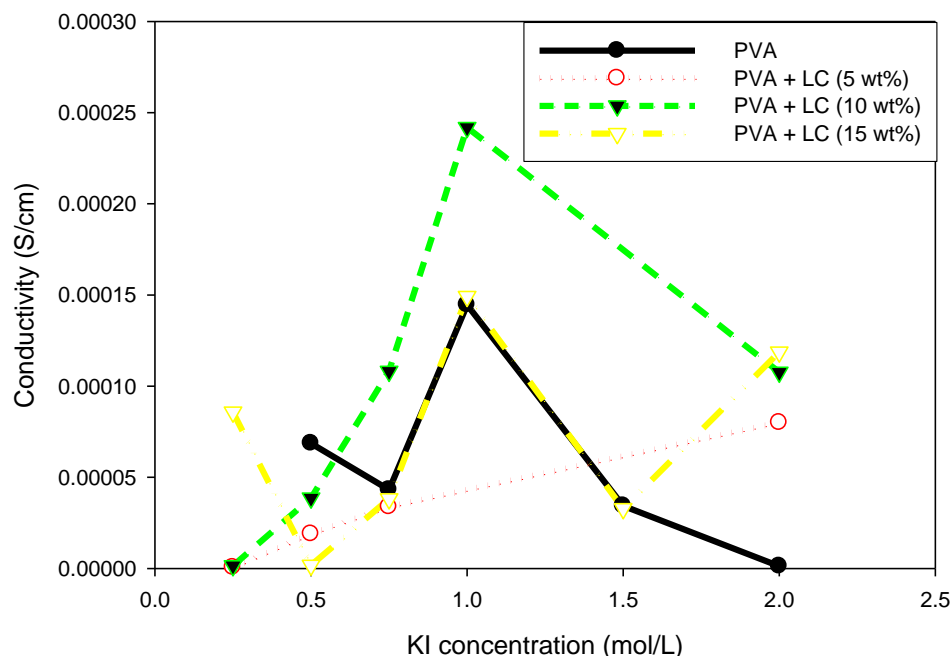

Figure 4.4 Variations of ionic conductivity at different LC and KI concentration

Figure 4.5 shows the ionic conductivity for different polymer electrolyte liquid crystal (PELC) system at different temperatures. The measurement was performed at room temperature up to 40 ºC for PELC membrane at 2 M KI solution. It can be seen from the curve that the ionic conductivity linearly increases with the increase with in temperature. This agrees well with the Arrhenius conductivity equation:

$$\sigma = (\frac{\sigma_0}{T})exp\left(\frac{E_a}{kT}\right)$$

where T is temperature in Kelvin, E_a is the activation energy and k is the boltzmann constant. The PELC with 15 wt% 5CB reached the highest ionic conductivity of 4.23 $\times$ 10^{-3} S/cm at 39ºC. This data also agrees well with the free volume model proposed by Miyamoto et al. (Miyamoto & Shibayama, 1973). According to the model, as the

temperature increases, the vibration of the polymer also increases until when the energy is high enough to push neighboring polymer chains which allows for the formation of void. Subsequently, the ions will fill in these voids and will move to the next aided by the segmental motion of the polymer chains. The increase in ionic conductivity can also be attributed to the decrease in viscosity as you increase the temperature which lead to the increase in flexibility of the polymer chains (Subba Reddy, Jin, Zhu, Mai, & Chen, 2006).
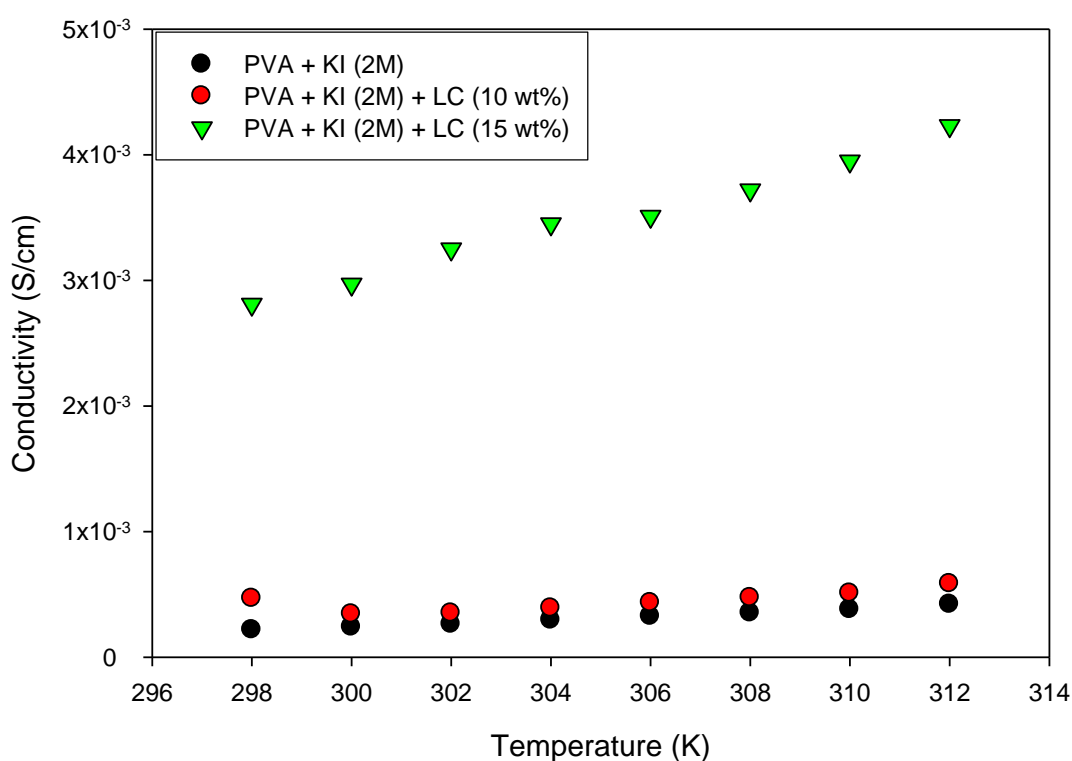

Figure 4.5 Variations of ionic conductivities at different temperatures

The above equation can also be used to determine the activation energy (E_a) by plotting the log σ versus 1000/T curve. The E_a is the minimum energy required to start the reaction, or in other words the energy required for defect deformation and migration where the defect is K^+ ions. A low E_a is ideal for generating a fast ionic hopping process. Figure 4.6 shows the variations of log σ with 1000/T. As can be seen from the curves, the increase in liquid crystal content lowers the activation energy. The polymer electrolyte with 15 wt% 5CB showed an activation energy of 1.130 eV where it also

correspond to the highest conductivity. This comparably low E_a indicates that the ion migration is easier with the inclusion of liquid crystal into polymer electrolyte.
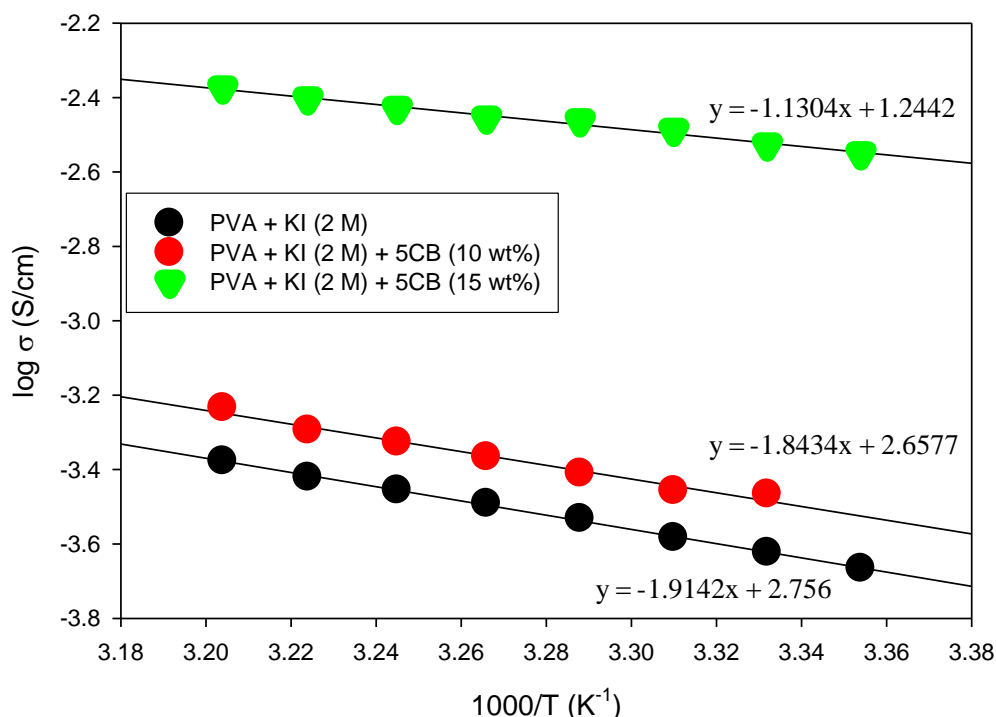

Figure 4.6 Plots of ionic conductivity versus 1000/T

Spin coating method

In this method, the conductivity of the sample was measured using the four point probe method where a curve below can be used to determine the resistance. As can be seen from the curve, at low frequency ($\sim$ 1 kHz), the sample behaves like a pure resistor. Thus the resistance value for the sample is taken as the average of the resistance from 1 Hz to 1 kHz.

The values of conductivities are given in Table 4.1. From the table, it can be seen that the conductivity reached highest conductivity of 7.82×10^{-4} S/cm at liquid crystal concentration of 5 wt%. Above the concentration, the conductivity began to decrease. This can be attributed to the increase viscosity within the polymer electrolyte which can impede the movement of ions.

Table 4.1 Conductivity result of spin coated sample

LC concentration (wt %)	Ionic conductivity (S/cm)
0	3.06×10^{-4}
5	7.82×10^{-4}
10	2.93×10^{-4}
15	1.22×10^{-4}
20	7.33×10^{-5}

*All samples contained PVA and KI (20 wt%)

Thermal analysis

DSC curve for a pure DSC is shown in the figure below (Figure 4.7). The glass transition temperature, T_g, is around 85 ºC. With the introduction of liquid crystal into the polymer electrolyte, the T_g decreases slightly to 78.88 ºC. The inclusion of the 5CB also decreases the crystallinity of the polymer and thus higher percentage of amorphous phase is present. This amorphous phase is important in allowing the ions to move freely within the polymer which increases the ionic conductivity.
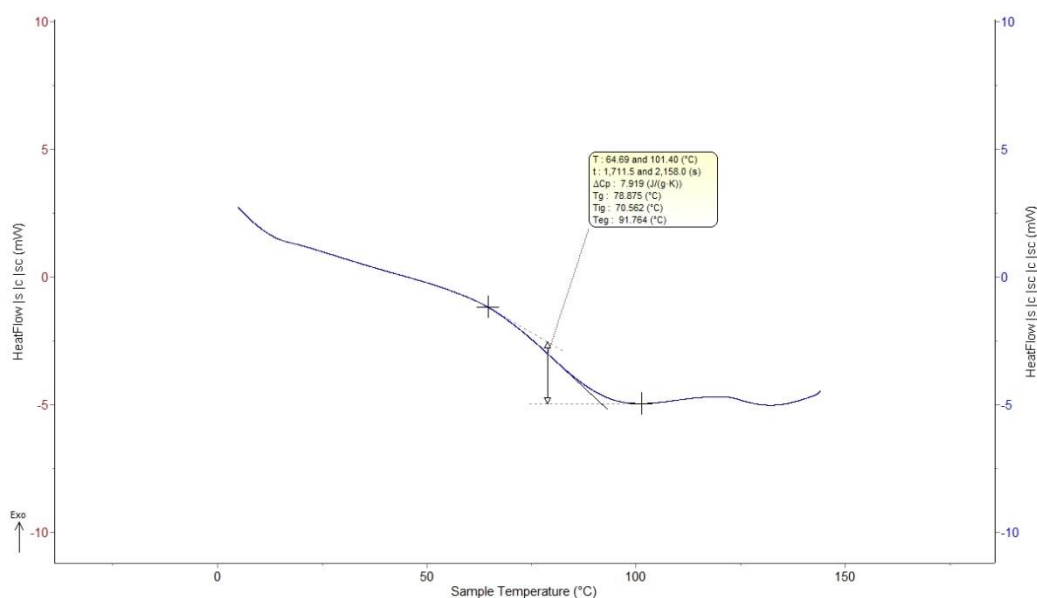

Figure 4.7 DSC thermogram of PVA+KI (20 wt%)+5CB (5 wt%)

Electrochemical analysis

The HOMO, LUMO and band gap energy can be determined from the CV curves using the following relations: $E_{HOMO} = - [E_{red} + 4.4]$ eV and $E_{LUMO} = - [E_{oxi} + 4.4]$ eV. The band gap can be calculated from the difference between E_{LUMO} and E_{HOMO}. Figure 4.8 shows the CV curves of the polymer electrolyte. Based on the cyclic voltammetry results, PVA+KI(20 wt%) shows $E_{HOMO} = - 6.933$ eV , $E_{LUMO} = - 5.275$ eV and $E_g = 1.657$ eV. On the other hand, PVA+KI(20 wt%)+5CB (5 wt%) shows $E_{HOMO} = - 6.588$ eV, $E_{LUMO} = - 5.031$ eV and $E_g = 1.557$ eV. A small amount of donor materials introduced into the polymer electrolyte create energy levels in the band gap near the conduction bad whereas a low level of acceptor materials will create band gap near the valence bad edge. With increase in the amount of doping, the density of states of these dopants increase and forms a continuum of states just like in the bands and effectively the band gap decreases (H. C. Casey & Stern, 1976). The presence of cyano group and alkyl group in 5CB also contributed to the narrowing of the band gap (Roncali, 2007).
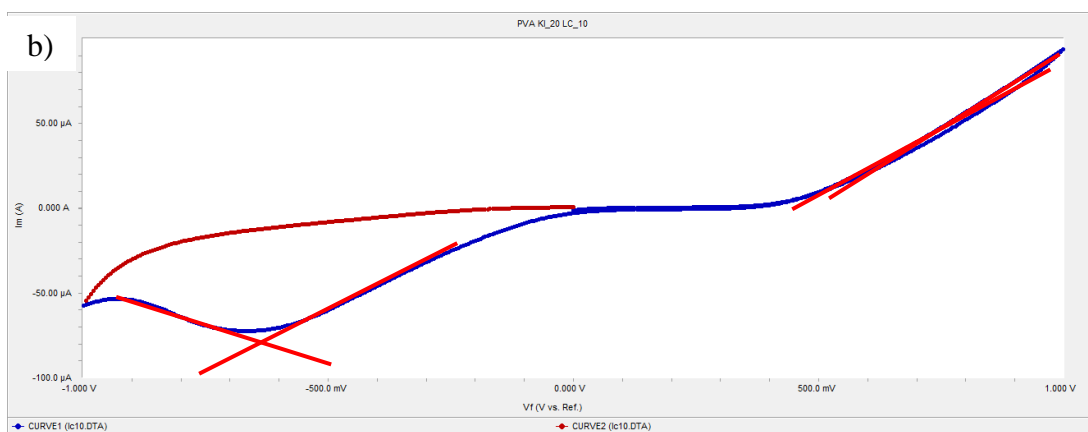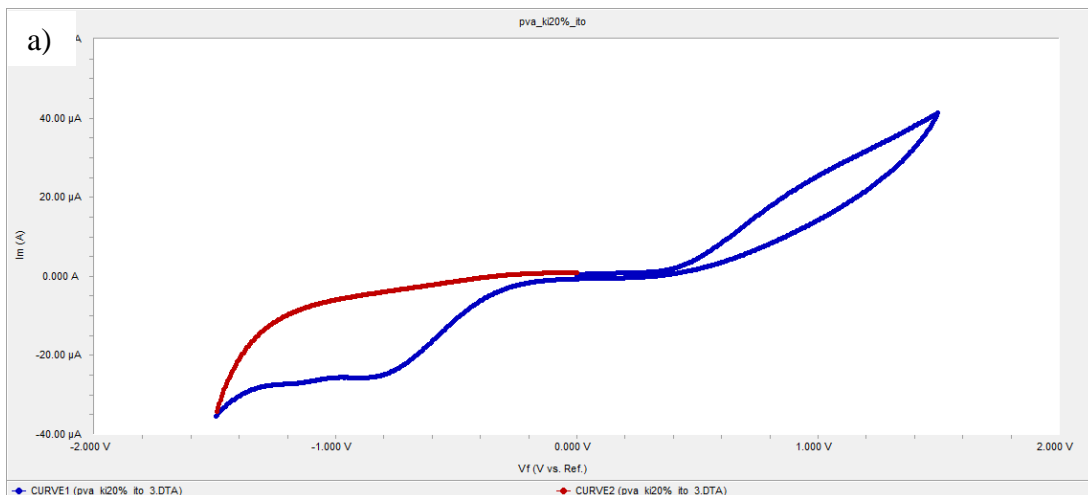
Figure 4.8 Cyclic voltammetry curves for a) PVA + KI (20 wt%) and b) PVA + KI (20 wt%) + 5CB (10 wt%)

CHAPTER 5

CONCLUSION

In summary, a series of polymer electrolyte incorporating liquid crystal was fabricated. The inclusion of the liquid crystal showed an increase in the ionic conductivity of the polymer electrolyte. The successful inclusion of the liquid crystal within the polymer electrolyte was verified by using optical polarizing microscope where the Schlieren structure of the liquid crystal embedded inside the polymer can be observed. To investigate the effect of the host polymer on the phase transition temperature of the liquid crystal, differential scanning calorimetry was used. The DSC curve also showed the effect of liquid crystal addition to the glass transition temperature, T_g, of the polymer host. The T_g can be related to the ionic conductivity where it is inversely proportional to the ionic conductivity. To investigate the possibility of the polymer electrolyte liquid crystal system to be used in solar cell applications, cyclic voltammetry experiment was performed where the band gap was determined. It is found out that the inclusion of the liquid crystal narrowed down the band gap. Overall, the result of this research shows the polymer electrolyte liquid crystal system resulted in a significant increase in conductivity and also the narrowing of the band gap which opened up possible applications for this material in solar cells and other energy conversion/storage devices.

CHAPTER 6

REFERENCES

Akagi, K., Piao, G., Kaneko, S., Sakamaki, K., Shirakawa, H., & Kyotani, M. (1998). Helical Polyacetylene Synthesized with a Chiral Nematic Reaction Field. *Science, 282*(5394), 1683-1686. doi: 10.1126/science.282.5394.1683

Bhattacharya, B., Lee, J. Y., Geng, J., Jung, H.-T., & Park, J.-K. (2009). Effect of Cation Size on Solid Polymer Electrolyte Based Dye-Sensitized Solar Cells. *Langmuir, 25*(5), 3276-3281. doi: 10.1021/la8029177

Bushby, R. J., & Lozman, O. R. (2002). Photoconducting liquid crystals. *Current Opinion in Solid State and Materials Science, 6*(6), 569-578. doi: http://dx.doi.org/10.1016/S1359-0286(03)00007-X

Chandra, S., Srivastava, B. B., & Khare, N. (1986). Liquid Crystal Assisted Photoelectrochemical Solar Cell With Chlorophyll Photoelectrode. *Molecular Crystals and Liquid Crystals, 132*(3-4), 265-274. doi: 10.1080/00268948608079547

Chen, K. F., Liou, C. H., Lee, C. H., & Chen, F. R. (2010, 20-25 June 2010). *Development of solid polymeric electrolyte for DSSC device.* Paper presented at the Photovoltaic Specialists Conference (PVSC), 2010 35th IEEE.

Debije, M. G., Piris, J., de Haas, M. P., Warman, J. M., Tomović, Ž., Simpson, C. D., . . . Müllen, K. (2004). The Optical and Charge Transport Properties of Discotic Materials with Large Aromatic Hydrocarbon Cores. *Journal of the American Chemical Society, 126*(14), 4641-4645. doi: 10.1021/ja0395994

Funahashi, M., & Hanna, J.-i. (2000). High ambipolar carrier mobility in self-organizing terthiophene derivative. *Applied Physics Letters, 76*(18), 2574-2576.

Funahashi, M., & Hanna, J. I. (2005). High Carrier Mobility up to 0.1 cm2 V-1 s-1 at Ambient Temperatures in Thiophene-Based Smectic Liquid Crystals. *Advanced Materials, 17*(5), 594-598. doi: 10.1002/adma.200401274

Gray, F. M. (1997). Polymer Electrolytes. *The Royal Society of Chemistry*.

H. C. Casey, J., & Stern, F. (1976). Concentration-dependent absorption and spontaneous emission of heavily doped GaAs. *Journal of Applied Physics, 47*(2), 631-643.

J.R. MacCallum, C. A. V. (1987). Polymer Electrolyte Reviews. *Elsevier*.

Kang, S. W., Jin, S. H., Chien, L. C., & Sprunt, S. (2004). Spatial and Orientational Templating of Semiconducting Polymers in a Cholesteric Liquid Crystal. *Advanced Functional Materials, 14*(4), 329-334. doi: 10.1002/adfm.200305083

Kim, H. K., Lee, M. J., Jin, S. H., & Lee, G. D. (2009). Optimization of Liquid Crystal Concentration in the Dye-Sensitized Solar Cell for High Efficiency. *Molecular Crystals and Liquid Crystals, 510*(1), 323/[1457]-1328/[1462]. doi: 10.1080/15421400903070283

Kim, J. H., Kang, M.-S., Kim, Y. J., Won, J., & Kang, Y. S. (2005). Poly(butyl acrylate)/NaI/I2 electrolytes for dye-sensitized nanocrystalline TiO2 solar cells. *Solid State Ionics, 176*(5–6), 579-584. doi: 10.1016/j.ssi.2004.10.002

Kim, J. H., Kang, M.-S., Kim, Y. J., Won, J., Park, N.-G., & Kang, Y. S. (2004). Dye-sensitized nanocrystalline solar cells based on composite polymer electrolytes containing fumed silica nanoparticles. *Chemical Communications*(14), 1662-1663.

M. R. Islam, R., Saidur, N. A. Rahim, K. H. Solangi. (2009). Renewable energy research in Malaysia. *Engineering e-Transaction, 4*(2), 69 - 72.

Manuel Stephan, A. (2006). Review on gel polymer electrolytes for lithium batteries. *European Polymer Journal, 42*(1), 21-42. doi: http://dx.doi.org/10.1016/j.eurpolymj.2005.09.017

Miyamoto, T., & Shibayama, K. (1973). Free-volume model for ionic conductivity in polymers. *Journal of Applied Physics, 44*(12), 5372-5376.

Nazeeruddin, M. K., De Angelis, F., Fantacci, S., Selloni, A., Viscardi, G., Liska, P., . . . Grätzel, M. (2005). Combined Experimental and DFT-TDDFT Computational Study of Photoelectrochemical Cell Ruthenium Sensitizers. *Journal of the American Chemical Society, 127*(48), 16835-16847. doi: 10.1021/ja052467l

Nogueira, A. F., Alonso-Vante, N., & De Paoli, M.-A. (1999). Solid-state photoelectrochemical device using poly(o-methoxy aniline) as sensitizer and an ionic conductive elastomer as electrolyte. *Synthetic Metals, 105*(1), 23-27. doi: http://dx.doi.org/10.1016/S0379-6779(99)00078-8

O'Regan, B., & Graetzel, M. (1991). A low-cost, high-efficiency solar cell based on dye-sensitized colloidal titanium dioxide films. *Nature, 353*(6346), 737-740.

Peter J. Collings, M. H. (1997). *Introduction to Liquid Crystals: Chemistry and Physics.*

Petritsch, K., Friend, R. H., Lux, A., Rozenberg, G., Moratti, S. C., & Holmes, A. B. (1999). Liquid crystalline phthalocyanines in organic solar cells. *Synthetic Metals, 102*(1–3), 1776-1777. doi: http://dx.doi.org/10.1016/S0379-6779(98)01035-2

Roncali, J. (2007). Molecular Engineering of the Band Gap of π-Conjugated Systems: Facing Technological Applications. *Macromolecular Rapid Communications, 28*(17), 1761-1775. doi: 10.1002/marc.200700345

Schmidt-Mende, L., Fechtenkötter, A., Müllen, K., Moons, E., Friend, R. H., & MacKenzie, J. D. (2001). Self-Organized Discotic Liquid Crystals for High-

Efficiency Organic Photovoltaics. *Science, 293*(5532), 1119-1122. doi: 10.1126/science.293.5532.1119

Shirakawa, H., Akagi, K., Katayama, S., Araya, K., Mukoh, A., & Narahara, T. (1988). Synthesis, Characterization, and Properties of Aligned Polyacetylene Films. *Journal of Macromolecular Science: Part A - Chemistry, 25*(5-7), 643-654. doi: 10.1080/00222338808053390

Subba Reddy, C. V., Jin, A. P., Zhu, Q. Y., Mai, L. Q., & Chen, W. (2006). Preparation and characterization of (PVP + NaClO4) electrolytes for battery applications. *The European Physical Journal E, 19*(4), 471-476. doi: 10.1140/epje/i2005-10076-8

Wang, H., Li, H., Xue, B., Wang, Z., Meng, Q., & Chen, L. (2005). Solid-State Composite Electrolyte LiI/3-Hydroxypropionitrile/SiO2 for Dye-Sensitized Solar Cells. *Journal of the American Chemical Society, 127*(17), 6394-6401. doi: 10.1021/ja043268p